Opt Rev (2015) 22:157–161
DOI 10.1007/s10043-015-0027-3

SPECIAL SECTION: SHORT NOTE

1st Optical Manipulation Conference (OMC'14), Yokohama, Japan

Binding of a pair of Au nanoparticles in a wide Gaussian standing wave

Lukáš Chvátal · Oto Brzobohatý · Pavel Zemánek

Received: 23 June 2014 / Accepted: 8 August 2014 / Published online: 25 February 2015

Abstract We present theoretical results related to the optical binding of two nanoparticles (NPs) in a standing wave created by a retro-reflected wide Gaussian beam. Recent experimental results demonstrated that this geometry enables easy confinement and spatial self-arrangement of NPs. Since the NPs are not usually of the same size, we investigate the influence of variations in NPs size on their stable spatial confinement in this type of optical trap.

Keywords Optical trapping · Standing wave · NPs · Optical binding

With the ongoing progress in the field of nanotechnology, controlled transport, manipulation and self-arrangement of individual NPs attract increased attention. Optical manipulation offers a way how to reach this goal in a contactless way even inside areas without mechanical access. Since the first demonstrations of spatial confinement of NPs using optical tweezers [1, 2] or a standing wave [3], optical manipulation techniques progressed tremendously [4–6] and the following techniques were mastered: spatial localization of NPs of various shapes and compositions [7–22], rotation of NPs [21, 23–26], NPs trapping in vacuum and their laser cooling [27, 28], NPs optical conveyor belts [29–31] and NPs optical separations [32–34].

Since the classical optical trap is at least one order of magnitude larger comparing to the NP size, several NPs can be illuminated at the same time. Illuminated NPs start to interact with each other via scattered light (so-called optical binding)[35] and tend to self-arrange into optically bound structures [36–47]. It was believed that optical binding between NPs is too weak to be observed, but recent results [48, 49] demonstrated that optical binding between metal NPs is much stronger and enables experimental observations. In this paper, we focus on a theoretical study how tiny deviations in the sizes of both NPs influence the stability of the formed optically bound structure in the geometry shown in Fig. 1.

L. Chvátal · O. Brzobohatý · P. Zemánek (✉)
Institute of Scientific Instruments, ASCR, Kralovopolska 147, 612 64 Brno, Czech Republic
e-mail: zemanek@isibrno.cz

1 Methods

Our calculations were performed using our own code based on the Generalized Lorenz–Mie theory with an extension to more spherical particles [50, 51]. Since we consider wide incident beam, the beam-shape-coefficients for the GBs were calculated according to the (first order) localized approximation [52] which corresponds to the first order Barton's correction of the GB [53]. For the numerical calculations in this paper, we consider the following parameters: GB waist radius $w_0 = 6.3\,\mu\text{m}$, total power in the incident GB at the sample plane $P = 100$ mW which gives optical intensity at the GB waist $I_0 = 2P/(\pi w_0^2) = 1.6$ mW/μm^2 and field intensity in GB waist $E_0 = \sqrt{4P/(\pi w_0^2 n_{\text{ext}} \varepsilon_0 c)} = 0.95$ V/μm, refractive index of the surrounding medium (water) $n_m = 1.33$, refractive index of Au $n_p = 0.285 + i7.35$ at the vacuum wavelength $\lambda_0 = 1064$ nm [54].

2 Nanoparticles of equal sizes

Since the NPs are of the same size, the problem is symmetrical and we expect that both NPs are symmetrically displaced with respect to the beam axis ($y_c = 0$). We

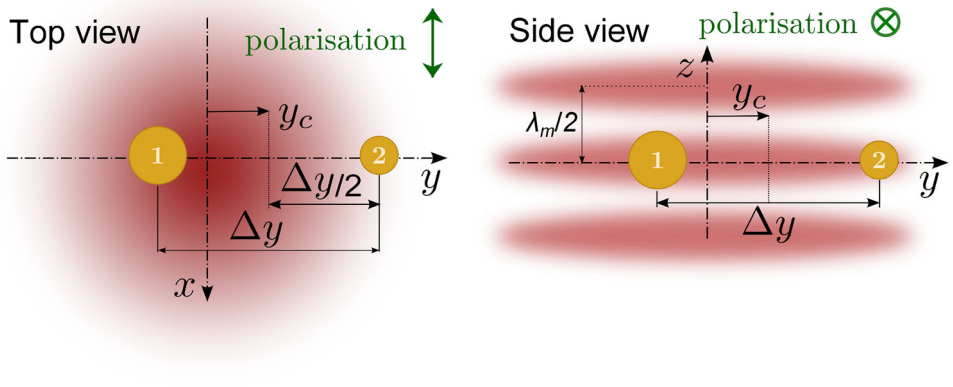

Fig. 1 (Color online) Geometry of the problem. *Top view* wide GB polarized along *x axis* illuminates two spherical NPs generally displaced asymmetrically from the beam axis. *Side view* The beam comes from the top against the direction of *z axis*, reflects backwards on the mirror and interferes with the incident beam forming a standing wave with fringes in the *xy* plane separated by one half of the trapping wavelength $\lambda_m/2$. The NPs are confined in the intensity maximum in the plane *xy*

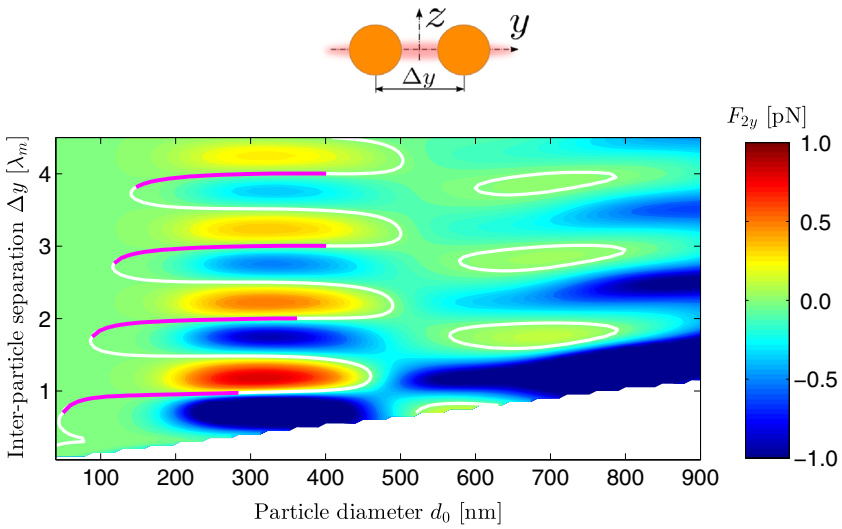

Fig. 2 (Color online) Maps of the optical force F_{2y} acting upon the right NP for different NP sizes and IPSs. The NPs are trapped only at the maximum of the interference fringes. The *magenta* sections denote $F_{2y} = 0$ with stable configurations along all axes

changed the NPs diameter and inter-particle separation (IPS) Δy and we looked for stable configurations of both NPs if they stay in the same *xy* plane. The equilibrium points were determined by zero values of all forces acting upon NP 1 and 2 along x, y, z axes. Further, at these points we evaluated the force stiffness matrix [55]

$$K_{ij} = -\frac{\partial F_i}{\partial q_j}, \tag{1}$$

$$\vec{F} = (F_{1x}, F_{1y}, F_{1z}, F_{2x}, F_{2y}, F_{2z}), \tag{2}$$

$$\vec{q} = (x_1, y_1, z_1, x_2, y_2, z_2), \tag{3}$$

using numerical derivatives equal to the 1st order central difference. The stable configurations must have all six eigenvalues of K, corresponding to six different vibrational modes, positive (in our sign convention).

Figure 2 shows the force F_{2y} acting upon the right NP. The stability analysis revealed that stable configurations occur only for smaller NPs trapped at the intensity maximum (magenta curves) and separated from each other by a number close to an integer multiple of the trapping wavelength in the medium, which corresponds to the observations [36, 48]. Larger NPs can be localized at the intensity minimum along z axis [56] but do not form stable optically bound structure (results not shown). Figure 2 also provides information about the magnitudes of the binding forces between NPs, extremal values are close to 1 pN for the considered parameters.

Figure 3 presents the results of the stability analysis along the stable configurations denoted by magenta curves in Fig. 2 for each of six vibrational eigenmodes. The stiffnesses $\kappa_{z\uparrow\uparrow}$ and $\kappa_{z\uparrow\downarrow}$ (green) are very high and both modes can not be distinguished because the intensity

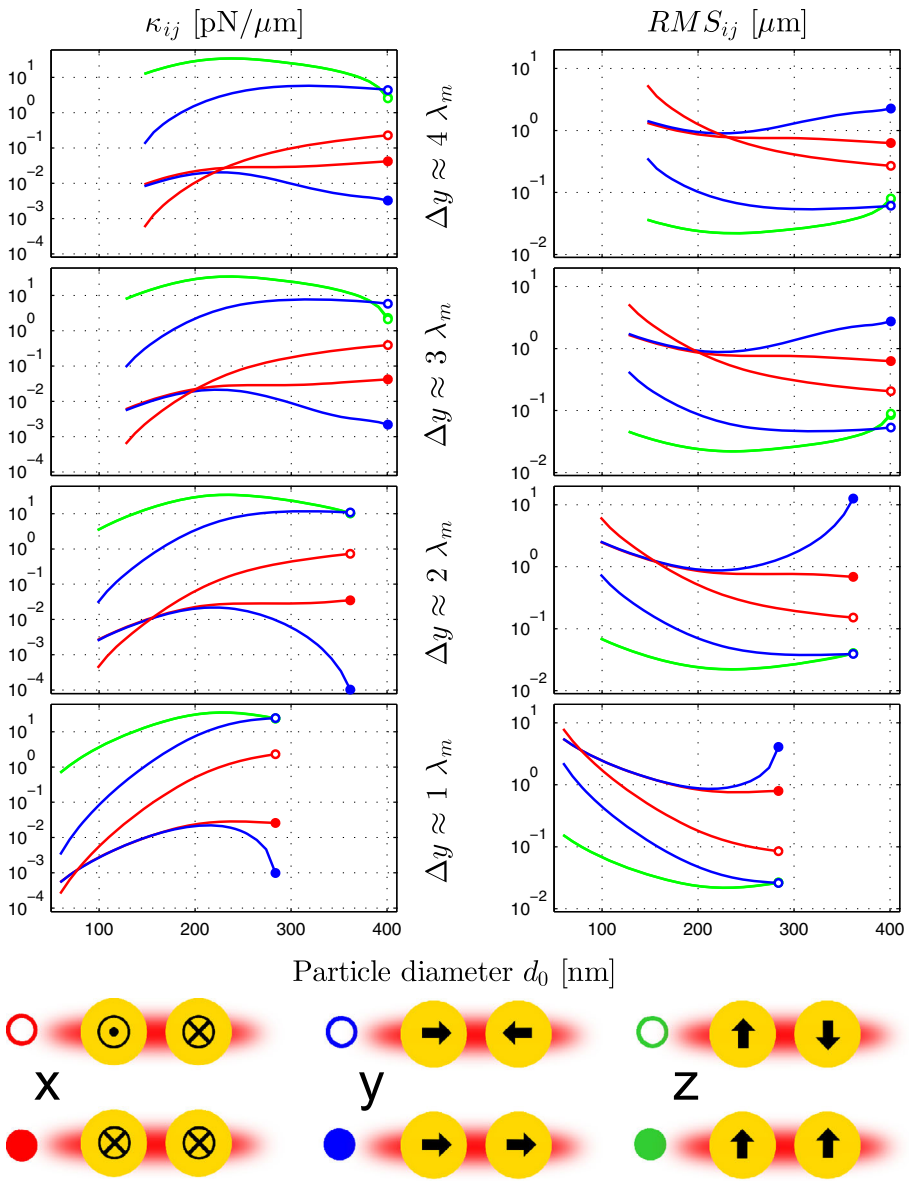

Fig. 3 (Color online) The *left column* shows the real values of the eigenvalues of K_{ij} from Eq. 1 corresponding to the optical stiffness κ_{ij} along i axis at the position of the right particle for each of parallel and antiparallel modes $j = \uparrow\uparrow$ and $j = \uparrow\downarrow$, respectively, denoted below the plots. The *right column* shows the corresponding root-mean-square displacements (RMS) of the right NP from the stable position for all six possible oscillations of both NPs. Each row corresponds to one stable IPS Δy. *Red*/*blue*/*green* colors denote vibrations along $x/y/z$ axis, *full*/*open circles* mark parallel/antiparallel vibration

gradient of the standing wave localizes the NPs very well within the single fringe (see $RMS_{z\uparrow\uparrow}$ and $RMS_{z\uparrow\downarrow}$ values) and their optical binding does not change this situation significantly. The stiffnesses $\kappa_{x\uparrow\uparrow}$ and $\kappa_{x\uparrow\downarrow}$ parallel to the beam polarization (red) are weak and almost the same for the smallest NPs. However they differ by several orders for larger NPs and get close to $\kappa_{z\uparrow\downarrow}$ demonstrating strong influence of optical binding. Stiffnesses along y axis are more interesting, $\kappa_{y\uparrow\uparrow}$ is very low and close to $\kappa_{x\uparrow\uparrow}$ because it is mainly done by the lateral intensity gradient of GB. However $RMS_{y\uparrow\uparrow}$ for considered power is close to Δy and thus, the optically bound structure would exist for higher trapping power. In contrast $\kappa_{y\uparrow\downarrow}$ approaches and even exceeds $\kappa_{z\uparrow\downarrow}$ for larger NPs with $RMS_{y\uparrow\downarrow} \ll \Delta y$. These results are in qualitative coincidence with astonishing results of Demergis [48].

Nanoparticles of different sizes. Analyzing this case, we assumed that the NPs are still aligned in xy plane and along y axis but they are not equally displaced from the beam axis. For the calculations we use the following parameters: IPS is done as $\Delta y = y_2 - y_1$ (see Fig. 1) and the shift of the NPs' geometry center from the beam axis we denote as $y_c = (y_1 + y_2)/2$.

NPs diameters d_1, d_2 are parametrized by a diameter d_0, and diameters ratio $p = d_1/d_2$ with $d_1 = d_0\sqrt{p}$, $d_2 = d_0/\sqrt{p}$. It is always assumed that the bigger NP is placed on the left (i.e. $z_1 < z_2$) having index 1, therefore, the parameter p is slightly larger than 1.

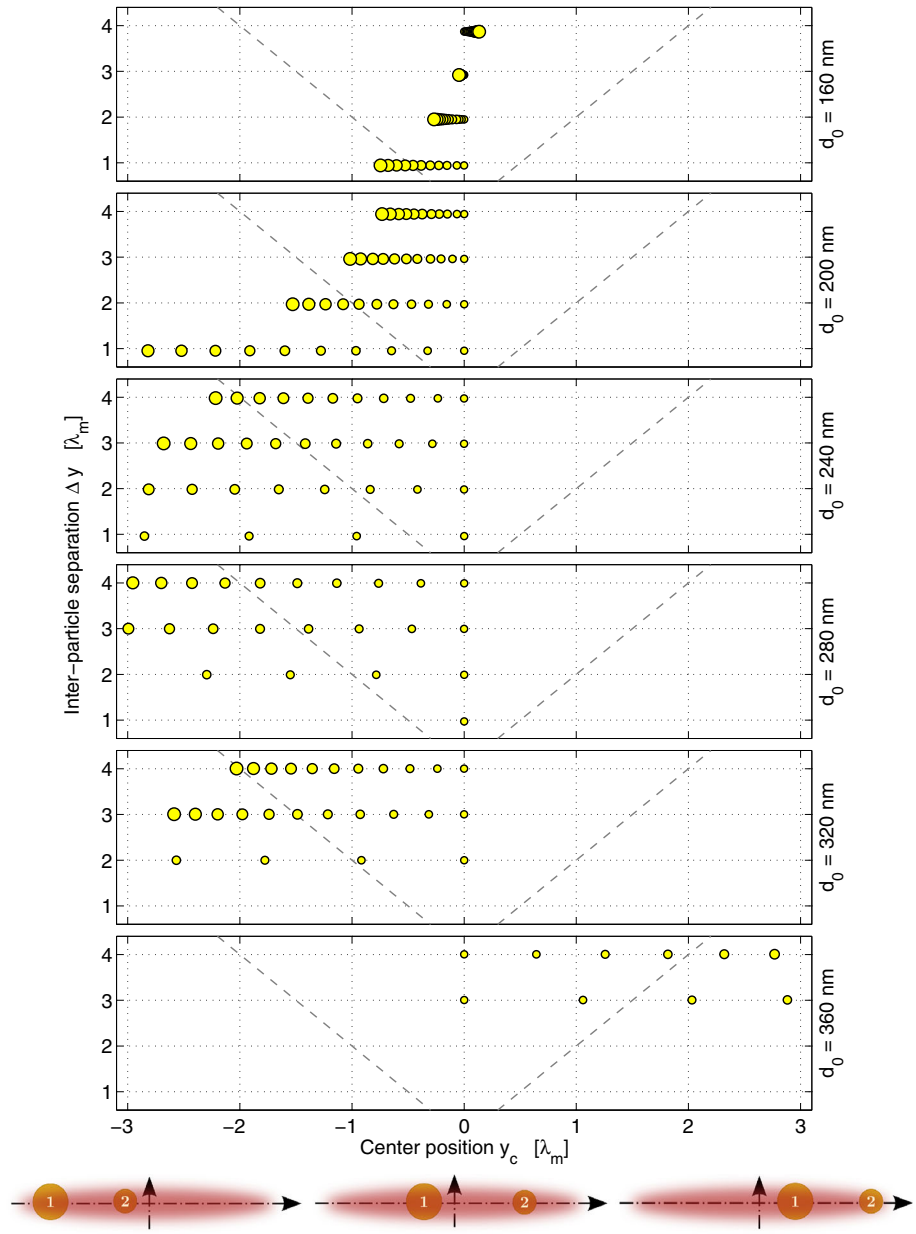

Fig. 4 (Color online) Stable configurations of two Au NPs of different radii along y axis. Eleven different marker sizes correspond to the growing ratio $p = 1 - 1.1$ in steps 0.1. Schemes on the bottom illustrates three possible configurations of the NPs with respect to the beam axis (and in the fringe intensity maximum) and correspond to the three regions in the plots separated by *dashed lines*

For several combinations of NPs diameters in the ranges d_0 =160–360 nm and p =1–1.1 we have calculated the optical forces F_1 and F_2 acting upon NPs 1 and 2, respectively, as functions of Δy, y_c, z, at $x = 0$. The equilibrium points were found from the calculated grid using a standard Matlab contouring algorithm which interpolates data between the grid points with higher than linear polynom. In the equilibrium points we evaluated the force stiffnesses according to Eq. 1 and determined the stable configurations.

Figure 4 reveals stable configurations found within the inspected range of NP parameters and geometry. With increasing difference in NP diameters the NPs are more displaced from the symmetrical configuration with respect to the beam axis. The larger IPS, the less the NPs are displaced from the beam axis. In majority of the studied cases, the NPs are shifted towards the side of the larger NP. Exceptions occur for the largest studied NPs that are shifted towards the side of the smaller NP and for the smallest NPs that are deviated to both sides depending on their IPS.

The presented results indicate that stable optically bound structures can be even formed from metal NPs of different sizes and one could deduce the ratio of their diameters from the deviation of a pair of optically bound NPs from the beam axis.

Acknowledgments The research was supported by CSF (project GA14-16195S), TACR (project TE01020233), and the research infrastructure by MEYS, EC, ASCR projects LO1212, CZ.1.05/2.1.00/01.0017, RVO:68081731, respectively.

References

1. K. Sasaki, M. Koshioka, H. Misawa, N. Kitamura, H. Masuhara, Appl. Phys. Lett. **60**, 807 (1992)
2. K. Svoboda, S.M. Block, Opt. Lett. **19**, 930 (1994)
3. P. Zemánek, A. Jonáš, L. Šrámek, M. Liška, Opt. Lett. **24**, 1448 (1999)
4. M. Dienerowitz, M. Mazilu, K. Dholakia, J. Nanophoton. **2**(021875), 1 (2008)
5. R. Quidant, C. Girard, Laser Photon. Rev. **2**, 47 (2008)
6. O.M. Maragò, P.H. Jones, P.G. Gucciardi, G. Volpe, A.C. Ferrari, Nat. Nanotechnol. **8**, 807 (2013)
7. K. Sasaki, J. Hotta, K. Wada, H. Masuhara, Opt. Lett. **25**, 1385 (2000)
8. P.M. Hansen, V.K. Bhatia, N. Harrit, L. Oddershede, Nano Lett. **5**, 1937 (2005)
9. C. Selhuber-Unkel, I. Zins, O. Schubert, C. Sönnichsen, L.B. Oddershede, Nano Lett. **8**, 2998 (2008)
10. J. Trojek, L. Chvátal, P. Zemánek, J. Opt. Soc. Am. A **29**, 1224 (2012)
11. J.K.C. Toussaint, M. Liu, M. Pelton, J. Pesic, M.J. Guffey, P. Guyot-Sionnest, N.F. Scherer, Opt. Express **15**, 12017 (2007)
12. M. Pelton, M. Liu, H. Kim, G. Smith, P. Guyot-Sionnest, N. Scherer, Opt. Lett. **31**, 2075 (2006)
13. C. Hosokawa, H. Yoshikawa, H. Masuhara, Phys. Rev. E **70**, 061410 (2004)
14. S. Ito, H. Yoshikawa, H. Masuhara, Appl. Phys. Lett. **80**, 482 (2002)
15. M. Dienerowitz, M. Mazilu, P.J. Reece, T.F. Krauss, K. Dholakia, Opt. Express **16**, 4991 (2008)
16. M. Righini, A.S. Zelenina, C. Girard, R. Quidant, Nat. Phys. **3**, 477 (2007)
17. L. Tong, V. Miljković, M. Käll, Nano Lett. **10**, 268 (2010)
18. J. Plewa, E. Tanner, D. Mueth, D. Grier, Opt. Express **12**, 1978 (2004)
19. F. Wang, W. Toe, W. Lee, D. McGloin, Q. Gao, H. Tan, C. Jagadish, P. Reece, Nano Lett. **13**, 1185 (2013)
20. M. Šiler, L. Chvátal, P. Zemánek, J. Quant. Spectrosc. Radiat. Transf. **126**, 84 (2013)
21. Z. Yan, J. Sweet, J. Jureller, M. Guffey, M. Pelton, N. Scherer, ACS Nano **9**, 8144 (2012)
22. Z. Yan, M. Pelton, L. Vigderman, E. Zubarev, N. Scherer, ACS Nano **7**, 8794 (2013)
23. P.H. Jones, F. Palmisano, F. Bonaccorso, P.G. Gucciardi, G. Calogero, A.C. Ferrari, O.M. Maragò, ACS Nano **3**, 3077 (2009)
24. K. Bonin, B. Kourmanov, T. Walker, Opt. Express **10**, 984 (2002)
25. P.V. Ruijgrok, N.R. Verhart, P. Zijlstra, A.L. Tchebotareva, M. Orrit, Phys. Rev. Lett. **107**(037401), 1 (2011)
26. A. Lehmuskero, R. Ogier, T. Gschneidtner, P. Johansson, M. Käll, Nano Lett. **13**, 3129 (2013)
27. J. Gieseler, B. Deutsch, R. Quidant, L. Novotny, Phys. Rev. Lett. **109 (2012)**
28. J. Gieseler, M. Spasenovic, L. Novotny, R. Quidant, Phys. Rev. Lett. **112 (2014)**
29. T. Čižmár, V. Garcés-Chávez, K. Dholakia, P. Zemánek, Appl. Phys. Lett. **86**, 174101 (2005)
30. M. Šiler, T. Čižmár, A. Jonáš, P. Zemánek, New J. Phys. **10**(113010), 1 (2008)
31. Y. Zheng, J. Ryan, P. Hansen, Y. Cheng, T. Lu, L. Hesselink, Nano Lett. **14**, 2971 (2014)
32. P. Zemánek, V. Karásek, A. Sasso, Opt. Commun. **240**, 401 (2004)
33. T. Čižmár, M. Šiler, M. Šerý, P. Zemánek, V. Garcés-Chávez, K. Dholakia, Phys. Rev. B **74**(035105), 1 (2006)
34. M. Ploschner, T. Čižmár, M. Mazilu, A. Di Falco, K. Dholakia, Nano Lett. **12**, 1923 (2014)
35. K. Dholakia, P. Zemánek, Rev. Mod. Phys. **82**, 1767 (2010)
36. M.M. Burns, J.-M. Fournier, J.A. Golovchenko, Science **249**, 749 (1990)
37. S.A. Tatarkova, A.E. Carruthers, K. Dholakia, Phys. Rev. Lett. **89**, 283901 (2002)
38. W. Singer, M. Frick, S. Bernet, M. Ritsch-Marte, J. Opt. Soc. Am. B **20**, 1568 (2003)
39. M. Šiler, T. Čižmár, M. Šerý, P. Zemánek, Appl. Phys. B **84**, 157 (2006)
40. C.D. Mellor, T.A. Fennerty, C.D. Bain, Opt. Express **14**, 10079 (2006)
41. P.J. Reece, E.M. Wright, K. Dholakia, Phys. Rev. Lett. **98**, 203902 (2007)
42. V. Karásek, O. Brzobohatý, P. Zemánek, J. Opt. A **11**, 034009 (2009)
43. O. Brzobohatý, V. Karásek, M. Šiler, L. Chvátal, T. Čizmár, P. Zemánek, Nat. Photon. **7**, 123 (2013)
44. O. Brzobohatý, T. Čižmár, V. Karásek, M. Šiler, K. Dholakia, P. Zemánek, Opt. Express **18**, 25389 (2010)
45. O. Brzobohatý, V. Karásek, M. Šiler, J. Trojek, P. Zemánek, Opt. Express **19**, 19613 (2011)
46. O. Brzobohatý, V. Karásek, T. Čižmár, P. Zemánek, Appl. Phys. Lett. **99**, 101105 (2011)
47. T. Čižmár, O. Brzobohatý, K. Dholakia, P. Zemánek, Laser Phys. Lett. **8**, 50 (2011)
48. V. Demergis, E.-L. Florin, Nano Lett. **12**, 5756 (2012)
49. Z. Yan, R.A. Shah, G. Chado, S.K. Gray, M. Pelton, N.F. Scherer, ACS Nano **7**, 1790 (2013)
50. Y.-L. Xu, Appl. Opt. **34**, 4573 (1995)
51. G. Gouesbet, G. Gréhan, *Generalized Lorenz-Mie Theories* (Springer, Berlin, 2011)
52. J.A. Lock, G. Gouesbet, J. Opt. Soc. Am. A **11**, 2503 (1994)
53. J.P. Barton, D.R. Alexander, J. Appl. Phys. **66**, 2800 (1989)
54. E. Palik, G. Ghosh, *Handbook of optical constants of solids*, vol. 3 (Academic Press, Waltham, 1998)
55. J. Ng, Z.F. Lin, C.T. Chan, P. Sheng, Phys. Rev. B **72**, 085130 (2005)
56. P. Zemánek, A. Jonáš, P. Jákl, M. Šerý, J. Ježek, M. Liška, Opt. Commun. **220**, 401 (2003)